

Photo- and electroluminescence behavior of biphenyl containing conjugated polymer

Tuğba KAYA DENİZ,¹ Doğukan Hazar APAYDIN,¹ Ali Can ÖZELÇAĞLAYAN,²
Levent Kamil TOPPARE,^{2,*} Ali ÇIRPAN²

¹Department of Polymer Science and Technology, Middle East Technical University, Ankara, Turkey

²Department of Chemistry, Middle East Technical University, Ankara, Turkey

Received: 22.02.2013 • Accepted: 22.04.2013 • Published Online: 12.07.2013 • Printed: 05.08.2013

Abstract: Light emitting properties of poly[4-(5-(biphenyl-4-yl)-4-hexylthiophen-2-yl)-2-dodecyl-7-(4-hexyl-thiophen-2-yl)-2H-benzo[d][1,2,3]-triazole] (PPhHTBT) and poly(9-vinylcarbazole) (PVK) blends were investigated with a configuration of ITO/PEDOT-PSS/BLEND/Ca/Al in ratios ranging from 5 to 100 wt% in PPhHTBT. Thin film and solution spectra of all blends revealed that energy transfer was completely achieved. Device performance increased for all blends and reached 1.1 cd/A for 30 wt% PPhHTBT.

Key words: Light emitting diode, photoluminescence, polymer blend, poly(9-vinylcarbazole)

1. Introduction

Recently, considerable research efforts have been dedicated to the development of electroluminescent polymers due to their numerous potential virtues such as low turn on and operating voltages, light weight, low-cost processing methods, and wide view angle.^{1–5} This concept was first reported by Burroughes et al. in 1990 with poly(p-phenylene vinylene).⁶ Electroluminescence (EL) is the process in which the recombination of an electron and a hole, which are injected by an external electrical field from respective electrodes, create an excited molecule that emits photons upon relaxation to the ground state.

In solid state, polymer chains tend to agglomerate due to the tendency to reduce surface energy. This usually causes the chains to aggregate, forming interchain excited states. Emission is broadened or diminished due to the formation of these interacting excited states (such as excimers or charge transfer excited states), which are competing with the intrinsic intrachain excited states for the capture of the excitons' energy.⁷ For the sake of a narrow band and highly efficient emission, this phenomenon can be avoided by isolating the chains to prevent the occurrence of interchain species that quench the fluorescence solid state films.⁸

Blending of semiconducting polymers is one of the methods proven to be effective in improving the photoluminescence (PL) and EL efficiency of PLEDs.^{9–13} This enhancement can be attributed to the significant suppression of interchain interactions.¹⁴ Blending the system with an inert polymer such as polystyrene or poly(methyl methacrylate) can enhance the emission efficiency of conjugated polymers by the dilution effect.^{15,16} However, the inert polymer may deteriorate the optical and electrical properties of the resulting polymer blend.

*Correspondence: toppare@metu.edu.tr

Dedicated to the memory of Professor Ayhan S. Demir

In addition to suppression of interchain species, careful selection of luminescent polymer blends or forming a host–guest system can be employed to increase emission efficiency. The host–guest system can be accomplished by doping a high energy emitting host (molecule with a broad band gap) with a low energy emitting guest (molecule with a narrow band gap), where excitation energies may be transferred under certain conditions from the higher energy host (donor) to the lower energy guest (acceptor).¹⁷ Forster energy transfer is one of these host–guest systems, in which energy transfer is established in a nonradiative manner.¹⁸

Furthermore, by blending the chromophore with an active polymer and controlling the energy transfer mechanism, emission can be tuned according to demand. Several studies have been conducted with this idea like white light generation through incomplete energy transfer between chromophores.^{19–21}

Poly(p-phenylene) (PPP) and its derivatives have been extensively investigated for use as light emitting materials as they are thermally and oxidatively stable polymers.^{22–25} The first blue emitting organic LED was achieved by PPP.²⁶ However, the low solubility of the material restricts its applicability.²⁷

In a previous study, we investigated the synthesis and electrochemical properties of a soluble biphenyl derivative, namely poly[4-(5-(biphenyl-4-yl)-4-hexylthiophen-2-yl)-2-dodecyl-7-(4-hexyl-thiophen-2-yl)-2H-benzo[d][1,2,3]-triazole] (PPhHTBT).²⁸ Herein, we examined the light emitting properties of PPhHTBT and its blends with poly(9-vinylcarbazole) (PVK).

2. Results and discussion

2.1. Optical properties

In order to observe the photophysical properties of the polymers, 10 mg/mL solutions of the polymers were prepared and spin coated on glass substrate at 1000 rpm for thin film absorbance and photoluminescence measurements. Furthermore, the solutions were prepared with a concentration of less than 10^{-5} M in order to prevent self-quenching for solution absorbance and photoluminescence measurements. In addition, the cell was degassed with nitrogen to prevent O₂ quenching of the emission during solution photoluminescence measurements. Solution and thin film absorption and emission spectra of PPhHTBT were investigated elsewhere.²⁸

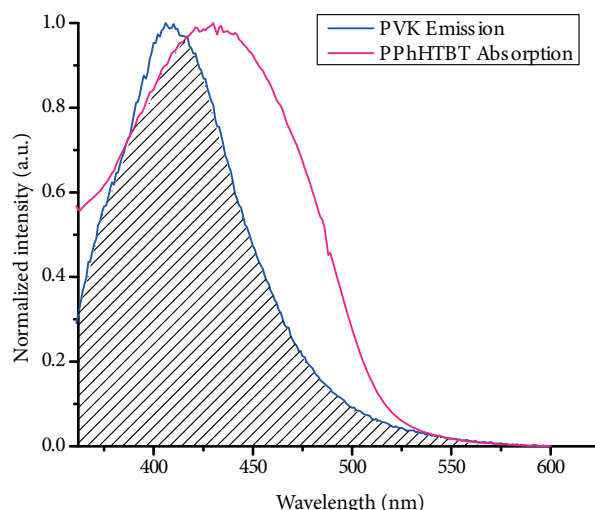


Figure 1. Spectral overlap of PVK emission and PPhHTBT absorption.

Figure 1 shows the absorption and emission spectra of films of PPhHTBT and PVK, respectively. PPhHTBT exhibits an interband $\pi - \pi^*$ transition at 430 nm and PVK shows an emission maximum at 410 nm, in agreement with the literature. The absorption spectrum of PPhHTBT overlaps with the emission spectrum of PVK in the range of 300–600 nm (signified by shaded region) as shown in Figure 1, which fulfills one of the basic requirement for efficient energy transfer.

Polymer blends were obtained by mixing PVK and PPhHTBT in chloroform with different weight ratios namely 5, 10, 20, 30, 40, and 100 wt% in PPhHTBT. Figures 2a and 2b show thin film and solution emission spectra for the blends excited at 370 nm.

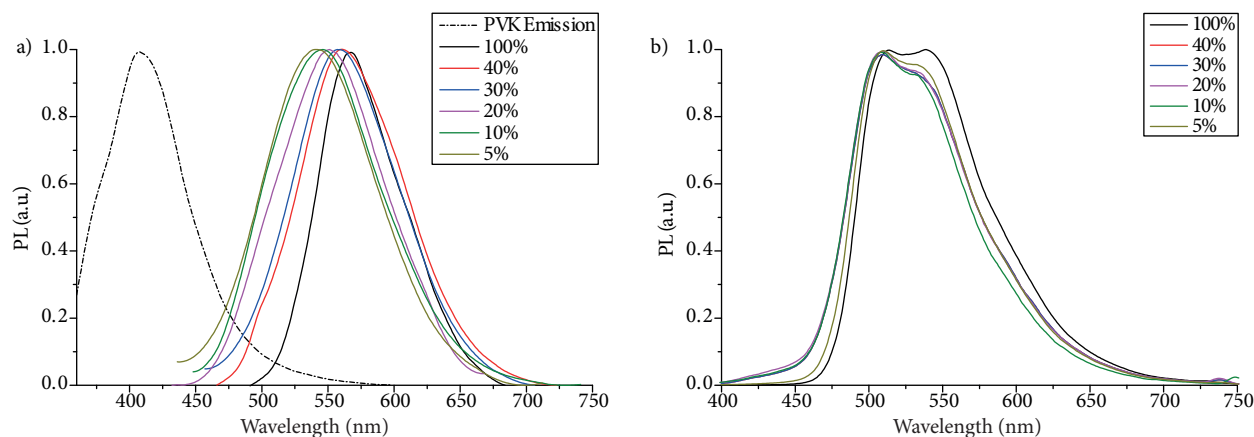


Figure 2. Thin film (a) and solution (b) fluorescence emission spectra of blends of PPhHTBT and PVK.

As can be seen from the thin film emission spectra (Figure 2a), even at very low concentration of the PPhHTBT (acceptor), no emission from the PVK (donor) was observed, which is an indication of complete energy transfer. The green light emitting polymer PPhHTBT reveals a peak at 567 nm that dominates the PL spectra of all blends. As the concentration of PVK increases, emission shifts to a shorter wavelength relative to the pure PPhHTBT solution emission spectrum. This is due to the dilution effect where PPhHTBT chains get more isolated by PVK matrix.

In order to analyze the energy transfer mechanism (Figure 2b), solution emission spectra of blends were studied. Unexpectedly, still no emission from the donor was seen even though it is known that for an efficient energy transfer close interaction should be provided for host and guest materials. For the pure polymer, the solution emission spectrum shows that emission occurs at 514 nm with a shoulder at 538 nm corresponding to the 0-0 and 0-1 transitions, respectively. The main peaks originate from single chain excitons, while the corresponding shoulders are established from interchain excitons.²⁹ As the concentration of the polymer is decreased, the blue portion of emission increases, while the red shoulder is seen to decrease with respect to pure polymer. Two factors contribute to this behavior. Firstly, isolation of the chains results in less aggregate states. Secondly, the higher energy emitting material (PVK) contributes more to the blue portion of the lower energy emitting material.

Comparison between solution and thin film emission spectra shows that polymer films were red-shifted by 30–40 nm from that of polymer solutions, indicating clearly that a stronger intermolecular interaction occurred in the solid state, which creates aggregates. These aggregates create lower energy interchain excited states in which excitons can be transferred through or quenched. Therefore, maxima of the emission red-shifted and the increased number of energy levels broadened the spectrum.

In addition, the observed vibronic fine structures in solution emission spectra disappeared in the thin film spectra due to the contribution of 2 factors. Firstly, the increase in the interchain species reduces the blue portion and increases the red portion of the emission. Secondly, as the concentration is increased, the 0-1 peak has less self-absorption loss because it is further from the absorption edge of the material than the main peak.³⁰ Emission maxima are summarized in Table 1. In order to further investigate the effect of dilution on energy transfer mechanism, 10- and 100-fold diluted emission spectra of the lowest (5%) and highest (40%) PPhHTBT concentration blends were taken (Figures 3a and 3b).

Table 1. Photophysical properties of blends.

PPhHTBT ratio	5%	10%	20%	30%	40%	100%
λ_{max}^{TF}	541	545	550	558	560	567
λ_{max}^{Soln}	508	509	509	510	511	514, 540

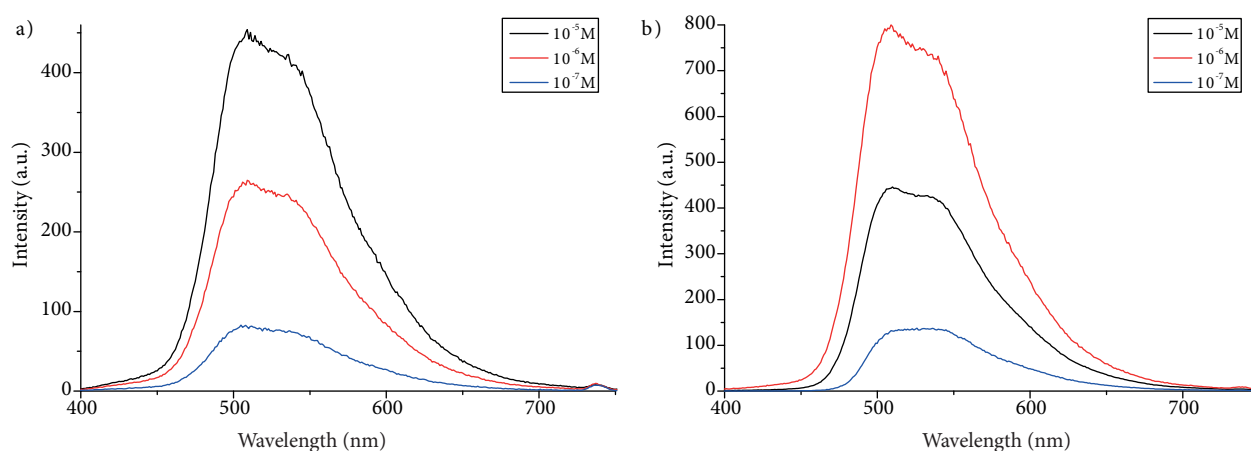


Figure 3. Solution emission of 40 (a) and 5 (b) weight percent of PPhHTBT in blend with PVK as a function of concentration.

It is seen from Figures 3a and 3b that the diluted spectra of both blends reveal similar behavior with respect to their concentrated spectra. However, as the distance between donor and acceptor increases, the contributed energy difference from donor to acceptor between the blue portion and the red portion of the emission decreases. This might be due to the fact that, as the donor and acceptor get away from each other, the importance of the energy transfers from the higher energy emitter (PVK) to the higher energy portion of the lower energy emitter (PPhHTBT) decreases. If we compare the effect of this proposal between 40% and 5% in PPhHTBT, it is seen that the higher concentration of acceptor is less affected, which has closer interaction with the donor.

Complete energy transfer from donor to acceptor, which seems to be prevalent even in the much diluted solutions state, indicates that these polymers are compatible and miscible in each other and that they do not need any additional process for better interactions, such as using surfactants.

2.2. Device properties

PLEDs of PPhHTBT/PVK blends were fabricated with a configuration of indium tin oxide (ITO)/poly(3,4-ethylene dioxythiophene)(PEDOT)/blend/Ca/Al with 5, 10, 20, 30, 40, and 100 wt% in PPhHTBT to test device characteristics.

Figures 4a and 4b show the luminance versus voltage and current density versus voltage curves for the devices. As seen in the figure, turn-on voltages are below 3 V. Below this voltage the current density reveals a linear increase with the voltage. This region is governed by thermally generated free charge carriers trapped in the bulk. As the voltage increases the traps get filled, and a sharp increase caused by further injected carriers is observed in the current density after 3 V. The hole injection barrier is much higher than the electron injection barrier for pure neat polymer as indicated in Figure 5. An unbalanced charge injection results in loss of efficiency, that is, injected electrons pass through the emitting region and reach the anode if they do not meet the holes. A hole transport layer PVK can reduce the imbalance charge injection. As seen from the J-V curves, electrons are trapped in PVK, needing more energy to reach the threshold voltage for the blends below 40% in weight of PPhHTBT. However, L-V curves show that the threshold voltage is decreased for the blends above 10% in PPhHTBT, meaning that more balanced injected charge carriers serve light output at lower voltages. As can be seen in Table 2, the efficiencies at luminance value of 200 cd/m² are increased for all blends and the necessary voltages for that luminance value are decreased for the blends up to 20%. The voltages are increased for the 5% and 10% blends due to the decrease in the average distance of excitons located on PPhHTBT chain segments between PVK segments. A low concentration of the material yields high distance and lower probability of the meeting of the charges. Still they reveal higher efficiencies compared to pure material because they need lower current values for achieving a luminance of 200 cd/m².

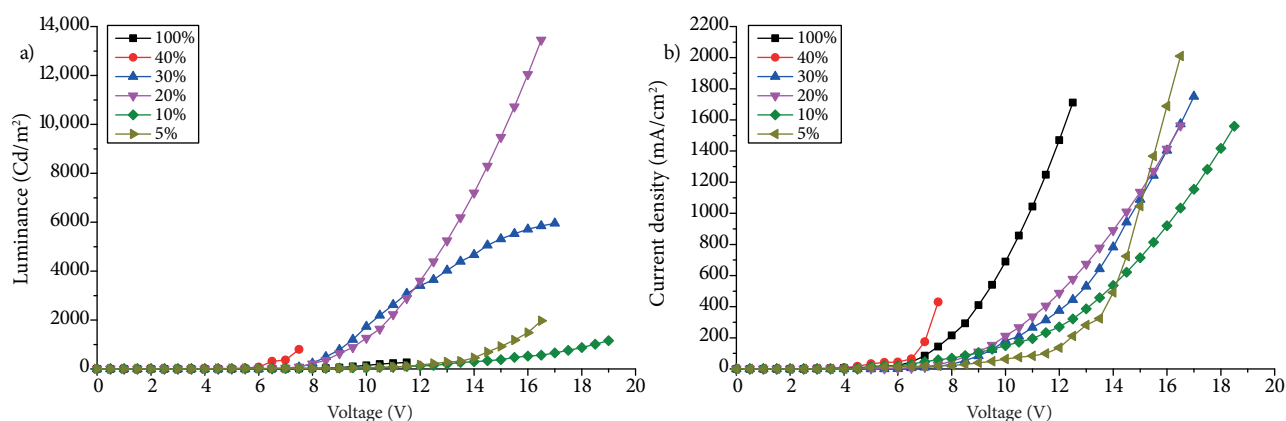


Figure 4. a) Luminance–voltage b) current density–voltage characteristics of ITO/PEDOT:PSS/emissive layer/Ca/Al.

Table 2. Device characteristics of PLEDs based on blends of PPhHTBT with PVK.

PPhHTBT ratio	5%	10%	20%	30%	40%	100%
λ_{max}^{EL}	508.2	510.4	510.6	511.6	513.4	558
Maximum luminance (cd/m ²)	1971 (16.5 V)	1158 (19V)	13453 (16.5 V)	2398 (12V)	796 (7.5V)	267 (11.5V)
Luminance Efficiency (cd/A)	0.6 (4.5V)	0.07 (18.5 V)	0.9 (16.5 V)	1.1 (10.5V)	0.55 (3V)	0.05 (3.5V)
Luminance Efficiency (cd/A)*	0.05	0.06	0.42	0.75	0.3	0.023
Turn on voltage (V)*	12.5	12	8	7.5	6	11
CIE	0.27,	0.29,	0.30,	0.32,	0.34,	0.39,
Coordinate (x,y)	0.52	0.53	0.55	0.56	0.54	0.54

*Values at 200 cd/m²

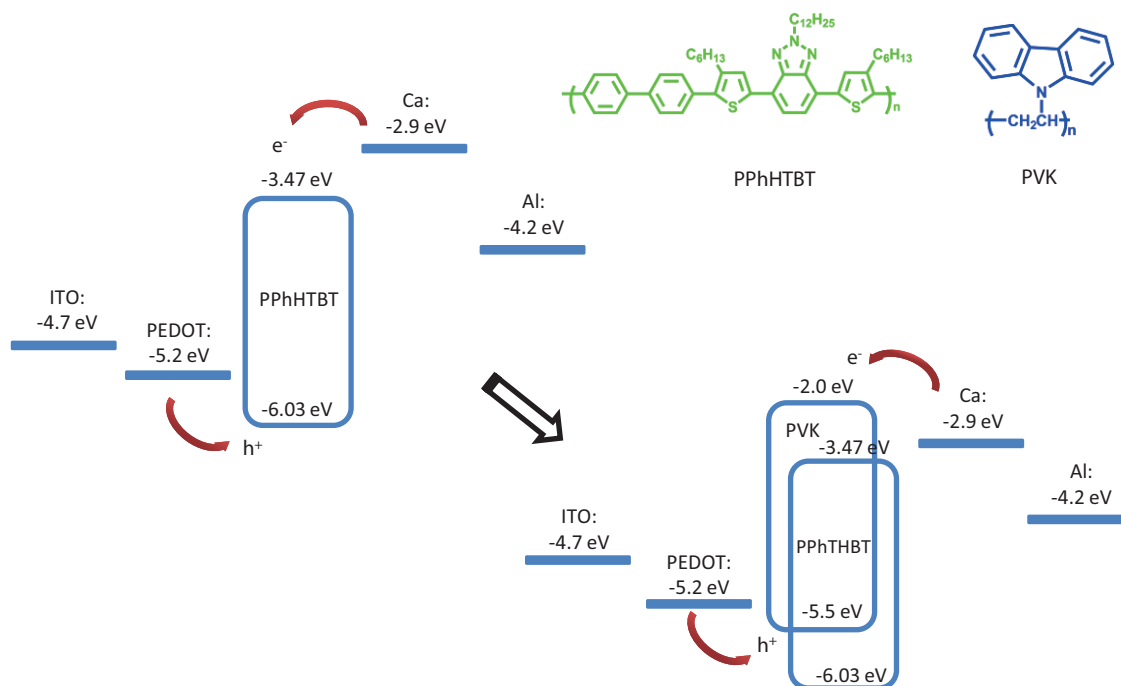


Figure 5. Schematic representation of chemical structures of the polymers and their energy levels.

EL spectra of polymer PPhHTBT and its blends with PVK are shown in Figure 6 and peak wavelengths are listed in Table 2. As in the case of PL spectra, no emission was observed from PVK, revealing that energy of the donor is transferred to the acceptor by either resonance coupling or charge transferring. As the concentration of the acceptor increased a small red-shift was observed for blends. However, there was a significant red-shift for the pristine device. This may be attributed to the dilution effect of PVK chains on PPhHTBT chains. The vibronic shoulder observed for 100 wt% blend disappears as the concentration decreases, which shows that the donor dominates more the higher energy region of the acceptor and due to the dilution effect fewer interchain species are created. In addition, the half width of the spectrum decreases from 95 nm to 80 nm from 100 to 5 wt% in PPhHTBT; this again gives information about less disordered microenvironment for the lower concentration of the acceptor.

The color of emission is highly dependent on blend ratio. Isolation of PPhHTBT decreases the importance of the green emission due to reduction in intra/interchain interaction of pure polymer, which leads to more red-shifted and lower energy emission. The color chromaticity diagram is shown in Figure 7 where the CIE chromaticity coordinates deviate to the blue emitting region as the percentage of the acceptor is decreased.

Energy transfer from donor to acceptor is related to the interaction distance and it is also dependent on the spectral overlap.³¹ As a result, more efficient energy transfer must be achieved as the acceptor concentration increases. However, aggregation and intermolecular chain interactions are increased as the concentration is increased, causing nonradiative excimer relaxation.³² Therefore, the effects of these 2 phenomena compete. It can be seen from the values given in Table 2 that the optimum concentration is achieved in 30% blend ratio, which possesses 1.1 cd/A luminance efficiency. This proves that the lower performance of low acceptor percentage blends compared to 30% can be attributed to the higher interaction distance. Moreover, the low performance of the higher acceptor percentage blend (40%) can be attributed to the aggregation states, probably even in phase separation, which results in emission quenching and increased interaction distance.

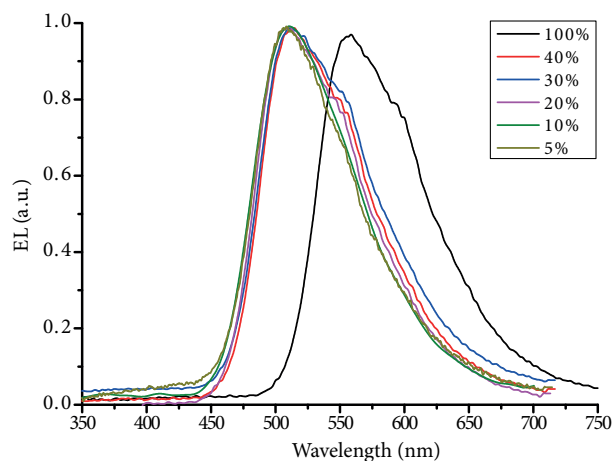


Figure 6. Electroluminescence spectra for each blend.

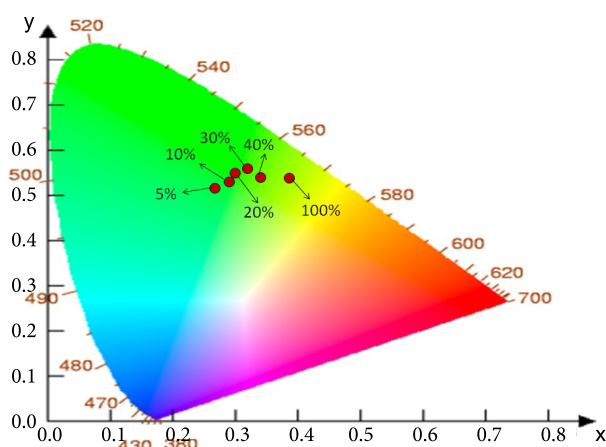


Figure 7. The CIE chromaticity diagram of all blends.

The PL spectra of the thin films shifted to the red region compared to their EL spectra. The difference between EL and PL spectra probably occurs due to the difference in the creation of the singlet excitons.³³ When blends are excited by means of photon absorption in the case of photoluminescence, the excitons are created on PVK. The excitons are transferred to the guest PPhHTBT in a nonradiative manner. Therefore, neutral excitons are formed directly on the polymer. On the other hand, the solution PL spectra of the blends show emission behavior very similar to that of EL spectra. This means that the relaxations in EL occur as if there is no aggregation between the chains and no quenching occurs. In other words, PVK behaved as a matrix for the polymer as well as an energy transfer component.

3. Experimental

3.1. Materials

All chemical reagents were purchased commercially and used without further purification except for THF. PVK (Aldrich), PEDOT:PSS (H.C. Stark), Al (Kurt. J. Lester), Ca (Kurt. J. Lester), and ITO (Visiontek Systems Ltd.) were used as received.

3.2. Synthesis

The synthesis of 4,7-bis(3-hexylthien-5-yl) 2-dodecyl-benzo[1,2,3]triazole (HTBT) was conducted according to the previous literature methods. The synthetic pathway for PPhHTBT was discussed in detail elsewhere. Polymerization was conducted via palladium(0) catalyzed Suzuki polycondensation reaction with equivalent molar ratios of dibrominated monomer (HTBT-Br) and diboronic ester substituted biphenyl under argon atmosphere. Molecular weight of the polymer is an important parameter that determines the degree of conjugation and interaction between the chains. A higher polydispersity index (PDI) introduces exciton traps since there is a distribution of band gaps. From GPC measurements PPhHTBT was found to have M_n of 8600 with a PDI of 3.8, which serves the purposes.²⁸

3.3. Electrochemical properties

The difference between the highest occupied molecular orbital (HOMO) and the lowest unoccupied molecular orbital (LUMO) values of the polymer determines the emission wavelength. In addition, positions of these values

are important since they determine the injection efficiency of the charges. Ideally the HOMO value should match the anode and the LUMO value should match the cathode for effective hole and electron injection, respectively. The HOMO and LUMO levels of the polymers were calculated from the onsets of oxidation and reduction potentials previously.²⁸

3.4. Thermal stability

The thermal properties of the PPhHTBT copolymer were investigated via thermogravimetry analysis (TGA) and differential scanning calorimetry (DSC) under nitrogen atmosphere. A 5% weight loss temperature was observed at 460 °C and 48% weight residue was observed at 800 °C, which are common for rigid polymers like PPP derivatives. The copolymer did not show any transition temperatures such as glass-transition temperatures (T_g) up to 400 °C, which originates from the rigid structure of the polymer. Lack of T_g up to high temperatures prevents morphological deformation and aggregational rearrangement that changes the optical properties of the material.

3.5. Device preparation

The PLED structures in this study were fabricated with the configuration of ITO/PEDOT:PSS/emissive layer/Ca/Al. ITO-coated glasses were purchased commercially with 2.5 cm × 2.5 cm dimensions. The specimen was etched and the middle of the specimen was masked with the help of vinyl tape. The nonmasked part of the specimen was etched with HCl and zinc dust. After that, the substrate was put in a 10% NaHCO₃ solution in order to neutralize the acid and the slide was washed with water. Finally, by immersing the ITO substrates into an ultrasonic bath they were washed with toluene, water and detergent, acetone, and isopropanol consequently for 15 min. The slides were cleaned by O₂ plasma treatment for further purifications. A thin film of hole transporting material PEDOT:PSS was formed on the slides by spin coating at 5000 rpm and annealed at 150 °C for 15 min. After that, PPhHTBT-PVK (10 mg/mL in chloroform) was prepared with different weight ratios by spin coating at 1000 rpm. The films were put into the vacuum chamber inside a nitrogen-filled glove box system (MBraun 200 B with moisture < 0.1 ppm, oxygen < 0.1 ppm) and 20-nm Ca cathode was deposited onto blend films. For preventing oxidation of the Ca, an 80-nm Al layer was deposited as a protecting layer. The shadow mask was designed such that 8 individual devices (active layer) with 0.06 cm² area were produced. After electrode deposition, the PLED devices were then encapsulated with glass and sealed with UV-cured epoxy glue in the glove box. Current-voltage-luminance and EL spectra measurements were conducted outside the glove box with a Keithley 2400 source meter and Maya 2000 spectrophotometer from Ocean Optics.

Acknowledgments

The authors appreciate the financial support from METU-BAP-01-03-2012-001 and thank METU Central Laboratory for the GPC, DSC, and TGA analyses.

References

1. Tang, C. W.; Van Slyke S. A. *Appl. Phys. Lett.* **1987**, *51*, 913–915.
2. Braun, D.; Heeger, A. J. *Appl. Phys. Lett.* **1991**, *58*, 1982–1984.
3. Kido, J.; Hongawa, K.; Okuyama, K.; Nagai, K. *Appl. Phys. Lett.* **1994**, *64*, 815–817.
4. Zhang, R.; Zeng, H.; Shen, J. *Synth. Met.* **1999**, *105*, 49–53.

5. Jiang, X. Z.; Liu, Y. Q.; Song, X. Q.; Zhu, D. B. *Synth. Met.* **1997**, *91*, 311–313.
6. Burroughes, J. H.; Bradley, D. D. C.; Brown, A. R.; Marks, R. N.; Mackay, K.; Friend, R. H.; Burn, P. L.; Holmes, A. B. *Nature* **1990**, *347*, 539–541.
7. Bernardo, G.; Charas, A.; Morgado, J. *J. Phys. Chem. Solids* **2010**, *71*, 340–345.
8. Yan, M.; Rothberg, L. J.; Papadimitrakopoulos, F.; Galvin, M. E.; Miller, T. M. *Phys. Rev. Lett.* **1994**, *73*, 744–747.
9. Alam, M. M.; Tonzola, C. J.; Jenekhe, S. *Macromolecules* **2003**, *36*, 6577–6587.
10. Cirpan, A.; Ding, L.; Karasz, F. E. *Polymer* **2005**, *46*, 811–817.
11. Yu, G.; Nishino, H.; Heeger, A. J.; Chen, T. A.; Rieke, R. D. *Synth. Met.* **1995**, *72*, 249–52.
12. Nishino, H.; Yu, G.; Heeger, A. J.; Chen, T. A.; Rieke, R. D. *Synth. Met.* **1995**, *68*, 243–247.
13. Cirpan, A.; Ding, L.; Kararsiz, F. E. *Synth. Met.* **2005**, *150*, 195–198.
14. Jakubiak, R.; Collison, C. J.; Wan, W. C.; Rothberg, L. J. *J. Phys. Chem. A* **1998**, *103*, 2394–2398.
15. Jung, H. J.; Park, Y. J.; Choi, S. H.; Hong, J.; Huh, J.; Cho, J. H.; Kim, J. H.; Park C. *Langmuir* **2007**, *23*, 2184–2190.
16. He, G.; Li, Y.; Liu, J.; Yang, Y. *Appl. Phys. Lett.* **2002**, *80*, 4247–4249.
17. Ragni, R.; Farinola, G. M. *Chem. Soc. Rev.* **2011**, *40*, 3467–3482.
18. Forster, T. *Ann. Phys.* **1948**, *2*, 55–75.
19. Niu, Q.; Xu, Y.; Jiang, J.; Peng, J.; Cao, Y. *J. Luminescence* **2007**, *126*, 531–535.
20. Zou, J.; Liu, J.; Wu, H.; Yang, W.; Peng, J.; Cao, Y. *Org. Electron.* **2009**, *10*, 843–848.
21. Deus, J. F.; Faria, G. C.; Faria, R. M.; Iamazaki, E. T.; Atvars, T. D. Z.; Cirpan, A.; Akcelrud, L. *J. Photochem. Photobiol. A–Chem.* **2013**, *253*, 45–51.
22. Edward A.; Blumstenge, S.; Sokolikb, P. I.; Yund, H.; Okamoto, Y.; Dorsinvilleb, R. *Synth. Met.* **1997**, *84*, 639–640.
23. Yang, Y.; Pei, Q.; Heeger, A. J. *Synth. Met.* **1996**, *78*, 263–267.
24. Chen, S. A.; Chao, C. I. *Synth. Met.* **1996**, *79*, 93–96.
25. Balanda, P. B.; Ramey, M. B.; Reynolds, J. R. *Macromolecules* **1999**, *32*, 3970–3978.
26. Grem, G.; Leditzky, G.; Ullrich, B.; Leising, G. *Adv. Mater.* **1992**, *4*, 36–37.
27. Ostergard, T.; Kvarnström C.; Stubb, H.; Ivaska, A. *Thin Solid Films* **1997**, *311*, 58–61.
28. Deniz, T. K.; Nurioglu, A. G.; Ünlü, N. A.; Sendur, M.; Toppare, L.; Cirpan, A. *Polymer* **2013**, *54*, 2243–2249.
29. Liu, J.; Shi, Y.; Yang Y. *Appl. Phys. Lett.* **2001**, *79*, 578–580.
30. McGehee, M. D.; Gupta, R.; Veenstra, S.; Miller, K. E.; Díaz-García, M. A.; Heeger, A. J. *Phys. Rev. B* **1998**, *58*, 7035–7039.
31. Eisenthal, K. B.; Siegel S. *J. Chem. Phys.* **1964**, *41*, 652–655.
32. Qiu, Y.; Duan, L.; Hu, X.; Zhang, D.; Zheng, M.; Bai, F. *Synth. Met.* **2001**, *123*, 39–42.
33. McGehee, M. D.; Bergstedt, T.; Zhang, C.; Saab, A. P.; O'Regan, M. B.; Bazan, G. C.; Srdanov, V. I.; Heeger, A. J. *Adv. Mater.* **1999**, *11*, 1349–1354.